Atmos. Chem. Phys. Discuss., 6, 4929–4971, 2006
www.atmos-chem-phys-discuss.net/6/4929/2006/

Atmospheric Chemistry and Physics Discussions

Measurement-based modeling of bromine chemistry in the boundary layer: 1. Bromine chemistry at the Dead Sea

E. Tas[1], M. Peleg[1], D. U. Pedersen[1], V. Matveev[1], A. Pour Biazar[2], and M. Luria[1]

[1]Institute of Earth Sciences, Hebrew University of Jerusalem, Israel
[2]Earth System Science Center, University of Alabama in Huntsville, Huntsvile, AL 35899 USA

Received: 13 February 2006 – Accepted: 8 March 2006 – Published: 19 June 2006

Correspondence to: E. Tas (erann@pob.huji.ac.il)

Abstract

The Dead Sea is an excellent natural laboratory for the investigation of Reactive Bromine Species (RBS) chemistry, due to the high RBS levels observed in this area, combined with anthropogenic air pollutants up to several ppb. The present study investigated the chemical mechanism of RBS at the Dead Sea using a numerical one-dimensional chemical model. Simulations were based on data obtained from comprehensive measurements performed at sites along the Dead Sea. The simulations showed that the high BrO levels measured frequently at the Dead Sea could only partially be attributed to the highly concentrated Br^- present in the Dead Sea water. Further, the RBS activity at the Dead Sea cannot solely be explained by a pure gas phase mechanism. This paper presents a chemical mechanism which can account for the observed chemical activity at the Dead Sea, with the addition of only two heterogeneous processes: the "Bromine Explosion" mechanism and the heterogeneous decomposition of $BrONO_2$. Ozone frequently dropped below a threshold value of ~1 to 2 ppbv at the Dead Sea evaporation ponds, and in such cases, O_3 became a limiting factor for the production of BrO_x (BrO+Br). The entrainment of O_3 fluxes into the evaporation ponds was found to be essential for the continuation of RBS activity, and to be the main reason for the positive correlation observed between BrO and O_3 at low O_3 concentrations, and for the jagged diurnal pattern of BrO observed in the Dead Sea area. The present study has shown that the heterogeneous decomposition of $BrONO_2$ has the potential to greatly affect the RBS activity in areas under anthropogenic influence, mainly due to the positive correlation between the rate of this process and the levels of NO_2. Further investigation of the influence of the decomposition of $BrONO_2$ may be especially important in understanding the RBS activity at mid-latitudes.

1 Introduction

It has become increasingly clear that Reactive Halogen Species (RHS) have the potential to significantly affect tropospheric chemistry (Von Glasow et al., 2004). This is due mainly to the fact that RHS can lead to boundary layer ozone destruction via catalytic chemical cycles. Several observations have detected a sharp depletion in boundary layer ozone concentrations, from normal values between 30 and 40 ppb to below detection limits (≤2 ppb) in the polar regions during springtime (Tuckermann et al., 1997; Hausmann and Platt, 1994; Barrie et al., 1988; Kreher et al., 1997; Murayama et al., 1992). It has been shown that elevated BrO levels of up to 30 ppt, are concurrent with episodes of boundary layer ozone destruction (Platt and Honinger, 2003).

It has also been recognized that RHS may also lead to boundary layer O_3 destruction at mid latitudes. This was first observed at the Dead Sea valley in Israel (Matveev et al., 2001; Hebestreit et al., 1999), based on an obvious anticorrelation between ozone and BrO during ozone depletion events. In these measurements, very high BrO levels above 150 ppt were detected together with daytime depletion of O_3 from levels greater than 120 ppb to below the detection limit of the instrument (≤2 ppb). Later, evidence for additional Reactive Bromine Species (RBS) activity was found at other mid-latitude locations, e.g., at the Great Salt Lake, Utah (Stutz et al., 2002), north of the Canary Islands (Leser et al., 2003) and at Salar de Uyuni, Bolivia (Honninger et al., 2004).

Previous research on RBS has been conducted either at the polar regions which have very low anthropogenic pollution levels or even pristine conditions (Ridley and Orlando, 2003; Tuckermann et al., 1997; Hausmann and Platt, 1994; Beine et al., 1997), or at mid-latitude locations with low concentrations of RBS (Stutz et al., 2002; Leser et al, 2003; Honninger et al., 2004). At the Dead Sea area very elevated concentrations of BrO (up to more than 150 pptv) are frequently observed (Tas et al., 2005), while in general, photochemical air pollution in this area can be characterized by average levels of NO_2 and SO_2 around several ppb. Therefore, the Dead Sea basin provides a unique natural laboratory for investigating the interaction between RBS and photochemical

pollutants.

The present study focuses on RBS activity in the Dead Sea area, Israel. The Dead Sea Valley, has unique geophysical conditions, being the deepest land area on the face of earth, situated about 400 m below sea level, between 31°00′ N and 31°50′ N–035°30′ E. The Dead Sea is one of the most saline lakes in the world with 5.6 g bromide/l and 225 g chloride/l (Niemi et al., 1997). The bromine content at the Dead Sea is higher than in normal ocean water (Sverdrup et al., 1942), higher than at the Great Salt Lake, Utah (Stutz et al., 2002) and Salar de Uyuni, Bolivia (Honninger et al., 2004) by factors of 86, 134, and 19 to 400, respectively. The Br/Cl ratio at the Dead Sea is higher than in normal ocean water and the Great Salt Lake, by factors of about 7.5 and 36, respectively. Both the relatively high bromine content and the high $[Br^-]/[Cl^-]$ ratio may be the fundamental reasons for the extremely high BrO levels that were measured at the Dead Sea. Based on the high measured Br^- content at the Dead Sea, it has been suggested that the "Bromine Explosion" mechanism may account for the high BrO levels measured at the Dead Sea (Tas et al., 2005, 2003; Matveev et al., 2001). Even so, the main chemical mechanisms that take place at this area were still unknown.

This paper is the first to present a chemical mechanism that can explain the fundamental chemical activity of RBS observed at the Dead Sea. This objective was achieved with a one dimensional model, which uses an explicit chemical mechanism, in combination with data obtained from comprehensive measurement campaigns. The present study focuses on the main factors and processes which lead to the efficient ozone destruction via BrO_x production, the extraordinarily high BrO levels, and the unique BrO diurnal profile obtained at the Dead Sea.

2 Experimental

2.1 Model description

The core of the research analysis was done by a one-dimensional Chemical Transport Model, UAHCTM_1D (Pour Biazar, 1995). This model includes an explicit gas phase chemical mechanism and takes into account the vertical motion of the different species based on diffusion and advection calculations and on deposition velocity values.

The model calculates the changes in the mixing ratio, C_i, of species i in the gas phase with time (t) according to Eq. (1):

$$\frac{\partial C_i}{\partial t} = -w\frac{\partial C_i}{\partial z} + \frac{\partial}{\partial z}\left[K_{(z)}\frac{\partial C_i}{\partial z}\right] + q_i + p_i - C_i l_i \quad (1)$$

where w is the vertical wind speed component, z indicates the vertical height, and $K_{(z)}$ is the exchange coefficient at height z. The two first right hand side terms are the advection and diffusion terms, respectively. q_i is the sum of emissions fluxes or advection fluxes for species i. p_i and $C_i l_i$ are the gas phase chemical production and loss, respectively. The fluxes through the top of the model, the surface emissions and the surface deposition flux are included in the model as boundary conditions of the second order partial differential equation term.

The basic photochemical processes described by 166 gas-phase reactions were based on the Trainer mechanism (Trainer et al., 1987), which was updated according to Atkinson et al. (2003). Thirty one reactions were added to describe the bromine gas phase mechanism (Tables 1 and 2). The deposition velocities of the bromine species that had a significant influence on the results of the present simulations are listed in Table 3. The velocities for NO, NO_2, C_4H_6O (methacrolien), C_4H_6O (methyl vinyl ketone) and PAN (peroxyacetyl nitrate) were calculated according to Trainer et al. (1987). Deposition velocities for H_2O_2, CH3OOH, $CH3O_2$ and CH_2O were calculated in the same way based on values from Sander and Crutzen (1996).

The rate constant for each photochemical reaction was calculated at a time resolution of 15 min by integrating over the relevant wavelengths, using Eq. (2):

$$k_p = \int_\lambda F(\lambda)\sigma(\lambda)\phi(\lambda)d\lambda \quad (2)$$

whereλ is the wavelength, ϕ is the quantum yield, σ is the absorption coefficient and F is the actinic flux. The actinic flux was calculated by running the Tropospheric Ultraviolet & Visible Radiation model (Madronich et al., 1998). All simulations were restricted to clear sky cases, based on global and ultraviolet radiation measurement data. The maximal error in actinic flux calculations is estimated to be 16% for the short UV range (<310 nm) and less for longer wave lengths.

Model simulations (as described later) could not duplicate the observed chemical effects of the bromine species without including two heterogeneous processes: (H1), the heterogeneous decomposition of $BrONO_2$ and (H2), the "Bromine Explosion Mechanism" (Fan and Jacob, 1992; Vogt et al., 1996; Mozurkewich et al., 1995; Tang and McConnell, 1996; Platt and Moortgat, 1999):

$$BrONO_2 + H_2O \rightarrow HOBr + HNO_3 \quad (H1)$$

$$HOBr + H^+ + Br^- \rightarrow Br_2 + H_2O \quad (H2)$$

These two reactions were entered into the model using parameterization for their first order rate constant, according to Eq. (3):

$$R = (\gamma < c > A)/4 \quad (3)$$

Where R is rate coefficient, γ is the uptake coefficient, $<c>$ is the mean thermal velocity and A is particle surface area per unit volume).

The basic physical assumptions are that Reaction (H1) takes place mainly on sulfate aerosols, while Reaction (H2) takes place mainly in the sea salt aerosols present over the water. The first assumption is based on the relatively high efficiency of the heterogeneous decomposition of $BrONO_2$ on sulfate aerosols (Von Glasow et al., 2002;

Hanson et al., 1996; Hanson and Ravishankara, 1995) together with the high levels of sulfate aerosols measured at the Dead Sea, averaging $\sim 8\,\mu g \cdot m^{-3}$. This value is very similar to other values that were reported for this area (Andrea et al., 2002; Wanger et al., 2000; Formenti et al., 2001).

Studies have shown that the dependence of the rate of Reaction (H1) on atmospheric conditions is essentially very weak (Hanson et al., 1996). The uptake coefficient for this reaction is only slightly dependent on particle size, composition of sulfuric acid, and temperature (Hanson et al., 1996; Hanson and Ravishankara, 1995). Further, the heterogeneous decomposition rate of $BrONO_2$ is very efficient under dry conditions (Hanson and Ravishankara, 1995), such as exist at the Dead Sea. The first order rate constant for Reaction (H1) was based on direct measurements of sulfate aerosol concentrations. A value of 0.75 was assumed for γ (H1) based on literature data (Atkinson et al., 2004; Hanson et al., 1996) and a comparison of model simulations with relevant measurements.

Previous studies have shown that Reaction (H2), the "Bromine Explosion", is the most probable chemical mechanism for the release of bromine into the gas phase at the Dead Sea (Matveev et al., 2001; Tas et al., 2005). In the present simulation study, it was assumed that Br_2 was released solely from the sea salt aerosols. This is not necessarily true, since it is also possible that part of the Br_2 is released directly from the water or salt surfaces (see later discussion, Sect. 3.1), or from sulfate aerosols (Von Glasow et al., 2002; Fan and Jacob, 1992). As supported by the model results, the release from sea salt aerosols is assumed to be the major contributor because there were very limited solid salt depositions in the investigation region.

Sea salt aerosol concentrations are a strong function of surface wind speed. Thus, this relationship was included in the parameterization of the rate of Reaction (H2), according to Eq. (4) (Gong et al., 1997; Gras and Ayers, 1983):

$$\ln \chi = \ln(b) + aU_{10} \tag{4}$$

where χ- ambient sea salt aerosol concentration; U_{10}- wind speed at 10 m height; a, b –

empirical parameters determined based on Gong et al. (1997). This parameterization was included mainly in order to examine its importance in the area under investigation.

The bromide concentrations in the sea water at the study site increases going from north to south, and thus different wind directions may have led to different BrO concentrations. The relation between wind direction and BrO concentrations was therefore analyzed based on measurements from the entire campaign. This analysis was based on the relation between wind direction and the magnitude $\overline{\mathrm{BrO}} \cdot \frac{n_t(i)}{n(i)}$, where $n_t(i)$ – time percentage in which positive BrO concentrations were measured for a wind direction (i); $n_{(i)}$ – time percentage during which wind direction (i) was measured during daytime; $\overline{\mathrm{BrO}}$ – average daytime BrO concentrations obtained for wind direction (i). This relation was parameterized into the rate of Reaction (H2).

The values for the rate of Reaction (H2) were normalized according to the adjustment of the simulations to measurements, including the parameterization of wind speed and wind direction. The average rate obtained for Reaction (H2) was $\sim 1.35 \cdot 10^{-6}$ ppb/s (as discussed later), in good agreement with reported values.

Fluxes for NO, NO_2 and 13 different hydrocarbons species, were entered into the model at heights between ground level and the base of the planetary boundary layer, based on actual measurements performed at the Dead Sea. The NO levels measured during the field campaigns were usually very low, and frequently dropped to below detection limits (0.1 ppbv) during BrO formation periods. Additionally, the effect of NO on the RBS mechanism in the model was observed to be of only secondary importance. Therefore, the role of NO is not discussed in this paper. A very small flux of Br_2 of $10\,molecules \cdot cm^{-2} \cdot s^{-1}$ was added for initiation of the bromine species activity, from ground level upwards, and ozone fluxes were added based on the criteria described later (Sect. 3.4).

Necessary meteorological parameters representative of real conditions were obtained by running the 1_d Meteorological model (McNider and Pielke, 1981). The meteorological conditions, fluxes, solar data and heterogeneous parameterizations were

updated every 15 min in all simulations.

2.2 Model simulations

Simulations were performed for 3 different days in August 2001 (4, 5 and 9, Julian days – 216, 217, 221) for which measurement data was available at the evaporation ponds. The measured BrO diurnal profiles during these days were representative of the entire campaign. The days chosen for simulations were those for which no significant signs for iodine species activity were detected. Since iodine oxide species formation has been detected at the Dead Sea (Zingler and Platt, 2005) it is important to perform the simulations only on those days without expected IO presence. The various conditions used in the simulations are summarized in Table 4.

During the simulations, the contribution of each reaction to the formation of its products was investigated by including an inert species as an additional product in the reaction. For example, Reaction (G1) appeared in the model as $Br+O_3 \rightarrow BrO+O_2+X$, where X is an inert gas product specific to Reaction (G1). The first derivative with time of the concentration of this inert species correlates with the rate of the reaction that produces this product, and appears in this paper as $\frac{\Delta[X]}{\Delta t}$, where X is the reaction number. The obtained magnitude, $\frac{\Delta[X]}{\Delta t}$, is the actual contribution of the reaction to the formation of its products, including the influence of atmospheric dynamic and deposition velocity of the products. Thus, this magnitude includes additional information than that obtained by direct calculation of the reaction rate. Another advantage is that it was calculated with the same time resolution as the model time step.

2.3 Field measurements

All simulations presented here were based on a comprehensive set of atmospheric trace gas measurements and relevant meteorological parameters collected at the Dead Sea. Continuous measurements of O_3, NO, NO_x, SO_2, particulate sulfates and nitrates, wind speed and direction, temperature, relative humidity, pressure and solar radiation,

were conducted at the evaporation ponds using the techniques described by Matveev et al. (2001) during 2–12 August 2001 (see Fig. 1 for site locations). The differential optical absorption spectroscopy (DOAS) technique was employed to quantify BrO (detection limit≤7 pptv) and NO_2 (detection limit≤0.5 ppbv) (Matveev et al., 2001). The continuous measurements were performed at the western edge of the ponds, while the DOAS measurements represent the average concentrations along a 5.8 km light path with the light source situated due east over the evaporation ponds.

During the continuous measurements, O_3 was detected by a monitor located at the western border of the evaporation ponds at the western end of the DOAS light path (Fig. 1). The O_3 monitor was located downwind of the DOAS reflectors, with wind vector and light path directions differing by less than about 20°. The changes in O_3 concentrations were detected with a time delay of about 10 to 30 min relative to the comparable changes in BrO levels, due to the transport of the air masses along the DOAS light path to the O_3 monitor. Thus, the measurements of BrO and O_3 represent concentrations in the same air mass at two different locations. In order to synchronize the measurements of ozone and BrO to the same time scale, the wind speed and direction were used to calculate the travel time along the DOAS light path, and the ozone measurements were adjusted back in time (Fig. 2a). All ozone concentrations presented in this paper have been adjusted in this way unless specifically stated otherwise.

Supporting parameters that were not available from the measurements performed at the evaporation pond site were obtained from other research campaigns performed at the Dead Sea. In Metzokei Dragot, a site some 400 m above the Dead Sea (see Fig. 1), NO_y species (NO_y=NO+HNO_3+2N_2O_5+NO_3+ organic nitrates + particulate nitrate +... (were detected by the use of an appropriate converter located before the inlet of the NO_x monitor. This, together with NO_2 data from the DOAS, was used to calculate the NOz ($NO=NO_y-NO_x$) concentrations. During another campaign at the Ein Bokek site canister samples were collected and analyzed for hydrocarbons using GCMS.

3 Results and discussions

3.1 Model verification

The measured BrO profiles at the Dead Sea are unique in their high concentrations, jagged shape and relationship to the measured ozone profile (Fig. 2a). While the basic relation between BrO and O_3 is of anti correlation, under certain circumstances, a positive correlation of O_3 to BrO can be seen (Fig. 2a). In order to confirm that the proposed chemical mechanisms used in the model accurately reproduce the RBS chemistry, these observations must also be reflected in the simulated diurnal profiles of BrO and O_3. The homogeneous mechanism could not correctly simulate the measured O_3 and BrO concentrations (Figs. 2a, b and 3). The simulated BrO profiles were less jagged and of lower magnitude than the measurements. Modeled O_3 showed a continuous decrease, was higher than actual values, and did not show the increases typical of the measured values. According to the model verification process described in this section, the addition of external ozone fluxes and heterogeneous processes to the basic homogeneous mechanism were both necessary in order to obtain a good fit between simulations and measurements.

3.1.1 Validation of ozone profiles

The general pattern of ozone levels measured at the evaporation ponds increased sharply at sunrise, and then began a steady decrease, reaching a minimum of nearly zero at around 11:00 a.m. After this point in time, however, a sharp increase in ozone occurred, alternating with sharp decreases, thus forming a pattern with a jagged shape (Fig. 2a). The "NOOZ" simulation did not capture the jagged ozone profile, even though heterogeneous reactions were included (Fig. 2b). The mid-day increases must be the result either of photochemical production or of advection from outside the area. The model showed that local photochemical production could not explain the observed increases in O_3 (Fig. 2b). Thus, these increases should be the result of the entrainment

of external air masses with higher O_3 concentrations into the area during periods of RBS activity. Due to the relatively small dimensions of the evaporation ponds at the Dead Sea (4 km East–West), this entrainment is possible, and may occur on a time scale of tens of minutes. Since the model used in this work is one dimensional, it cannot account for external advection of chemical species, and it was, therefore, necessary to add horizontal O_3 fluxes during the simulations. The O_3 fluxes were entered into the model with a time resolution of 15 min, based on the measured O_3, and on changes of modeled Br concentrations with time (Sect. 3.4). The process by which ozone fluxes are entrained into the evaporation ponds, their influence on the RBS activity, and their relation to Br concentrations are discussed in detail in Sect. 3.4.

The inclusion of advected ozone fluxes in the model led to a good agreement between the trends in the simulations and measurements of ozone (Fig. 2c) during periods of intensive RBS activity (i.e, 08:00–18:00). The simulated ozone concentrations were approximately 3-fold lower than the measured ozone (Fig. 2b). However, it is not necessary to obtain strict agreement between the two, because, in general, the crucial factor in determining the correct BrO profile is the timing of the changes in ozone levels, rather than their magnitude. The BrO concentrations were generally found to be relatively insensitive to the magnitude of the ozone levels, unless the ozone crossed a threshold value of about 1 to 2 ppb (Figs. 2a, c), as explained in Sect. 3.4.

As stated above, a reasonable agreement between the measured BrO profiles and the simulations can be had with only a rough similarity in measured and simulated ozone levels. Furthermore, the difference between the measurements and the simulations is most likely an overestimation, considering that the O_3 measurements were conducted at the edge of the evaporation ponds. Since the concentrations of RBS are expected to be lower at the edge of the evaporation ponds than over the ponds, the measurements would not capture the full O_3 destruction, and this assumption may partly explain why the measured O_3 levels are higher than the simulated ozone levels.

3.1.2 Validation of BrO profiles

As stated previously, even after including ozone advection into the region, the simulations could not emulate the unique BrO profile without including two heterogeneous processes (Reactions H1 and H2). This can be seen in Fig. 3, which shows simulations without Reaction (H2) (NOH2), without Reaction (H1) (NOH1), and with both reactions (FULL). It should be noted that the simulations, except for FULL, were initiated with a Br_2 flux about 10^9 times higher than normal simulation fluxes (Table 4). This Br_2 flux was unrealistically high, and was necessary in order to get reasonable results. Even though the addition of Reaction (H1) produces the typical BrO diurnal pattern, it is only when both of the heterogeneous reactions are added together (FULL simulation) that the simulations agree with both the BrO pattern and its magnitude (Fig. 3). The simulated results were relatively insensitive to the parametrization of wind speed, suggesting that the rate of Reaction (H2) depends only weakly on concentrations of sea salt aerosols. This may imply that the sea salt aerosols are not the only source of airborne Br, and that Br may be released directly from the seawater or from salt pans by Reaction (H2). Similarly, the model simulations were also insensitive to the parameterization of wind direction.

Following the good agreement obtained for 9 August (Julian day 221), the entire FULL simulation was performed for two other representative days, 4 and 5 August (Julian days 216 and 217). Good agreement between simulations and measurements was obtained for the three days, indicating that with the inclusion of advected O_3 fluxes and two heterogeneous processes, the model is capable of relative accuracy and reproducibility in predicting BrO formation (Fig. 4).

3.2 Chemical mechanisms

Several field campaigns and laboratory investigations have shown that halogen atoms and their oxide radicals are key species in the chemical mechanisms responsible for the destruction of ozone (Barrie and Platt, 1997; Tuckermann et al., 1997; Wayne et

al., 1995; Matveev et al., 2001). A number of studies (Hebestreit et al., 1999; Matveev et al., 2001) performed at the Dead Sea have clearly shown the role of BrO_x (BrO+Br) in causing ozone depletion. Two main chemical mechanisms have been proposed as being responsible for the catalytic destruction of ozone at the boundary layer.

The first mechanism is driven by the self reaction of BrO and the photolysis of Br_2:

Cycle 1 (BrO-cycle)

$$Br_2 + h\nu \rightarrow 2Br \quad \text{(GP1)}$$

$$Br + O_3 \rightarrow BrO + O_2 \quad \text{(G1)}$$

$$BrO + BrO \rightarrow 2Br + O_2 \quad \text{(G2)}$$

$$\rightarrow Br_2 + O_2 \quad \text{(G3)}$$

$$2O_3 \xrightarrow{BrO_x} 3O_2$$

The second mechanism is initiated by the hydroperoxyl radical as shown below:

Cycle 2 (HOBr-cycle)

$$BrO + HO_2 \rightarrow HOBr + O_2 \quad \text{(G6)}$$

$$HOBr + h\nu \rightarrow OH + Br \quad \text{(GP3)}$$

$$Br + O_3 \rightarrow BrO + O_2 \quad \text{(G1)}$$

$$HO_2 + O_3 \xrightarrow{HOBr,BrOx} OH + 2O_2$$

As long as O_3 concentrations are higher than ∼1 to 2 pbbv, the rate limiting steps in the above cycles are Reactions (G2) and (G6). It should be noted that the efficiency of Cycle 2 is linearly dependent on the BrO concentration whereas the BrO dependence of Cycle 1 is quadratic. Thus, at high BrO levels, such as observed at the Dead Sea (Matveev et al., 2001), Cycle 1 should dominate.

All measurement campaigns performed at the Dead Sea (Tas et al., 2005; Matveev et al., 2001; Hebestreit et al., 1999; Stutz et al., 1999) have shown the presence of elevated BrO levels. As described above, heterogeneous processes are required in order to simulate the observed BrO_x production. Cycle 3, especially Cycle 3b, is suggested (Sects. 3.5 and 3.6) as being the chemical mechanism which promotes the extensive BrO_x production at the Dead Sea:

Cycle 3

$$BrO + NO_2 \xrightarrow{M} BrONO_2 \quad \text{(G14)}$$

$$BrONO_2 + H_2O \rightarrow HOBr + HNO_3 \quad \text{(H1)}$$

A B

$$HOBr \xrightarrow{h\nu} OH + Br \quad \text{(GP3)} \qquad HOBr + H^+ + Br^- \rightarrow Br_2 + H_2O \quad \text{(H2)}$$

$$Br_2 \xrightarrow{h\nu} 2Br \quad \text{(GP1)}$$

$$Br + O_3 \rightarrow BrO + O_2 \quad \text{(G1)}$$

net: Cycle 3a

$$NO_2 + H_2O + O_3 \xrightarrow{BrO_x} HNO_3 + OH + O_2$$

Cycle 3b

$$O_3 + NO_2 \xrightarrow{H^+,Br^-,BrO_x} Br + HNO_3 + O_2$$

Cycle 3 includes the heterogeneous decomposition of $BrONO_2$ via Reaction (H1) followed either by the photodissociation of HOBr to Br (Reaction GP3) (Cycle 3a) or by the release of Br_2 by the "Bromine Explosion" mechanism (Reaction H2) followed by the photolyzation of Br_2 to yield 2Br (Reaction GP1) (Cycle 3b). Cycle 3 is then completed by the reformation of BrO from the reaction of Br with O_3 (Reaction G1).

3.3 The RBS activity at the Dead Sea

The suggested RBS mechanism for the Dead Sea evaporation ponds area is schematically displayed in Fig. 5, while the diurnal profiles of some important bromine containing species obtained during "FULL" simulation are shown in Fig. 6. A sharp increase in HOBr occurs during the evening time (18:00–20:00) since the photolysis rate of HOBr decreases drastically during this time and because at the Dead Sea, the rate of decomposition of Reaction (H1) is much greater than the rate of Reaction (H2), (Sect. 3.6). It can be seen that during RBS activity, BrO is not the only species that has a jagged diurnal profile and according to the model simulations other bromine species have a similar jagged shape. It should also be remarked that the concentrations of OBrO are very small relative to the other bromine species and for this reason the OBrO can hardly be observed in the graph.

3.4 O_3 depletion, BrO profiles and O_3 fluxes

One important finding of the present study is that at the Dead Sea, O_3 can occasionally function as a limiting factor in the formation and recycling of BrO_x and the consequent

O_3 destruction. This can be understood due to the fact that the catalytic destruction of tropospheric O_3 by RBS can be described by Cycles 1, 2, 3a and 3b. In these cycles, Reaction (G1) influences the rate of O_3 destruction only if O_3 levels drop below ∼1 to 2 ppb. Thus, the rate of ozone destruction via BrO_x production and recycling through these cycles is not normally dependent on its own concentrations, unless O_3 levels drop below ∼1 to 2 ppbv, as occasionally observed in the Dead Sea area. The proper treatment of O_3 fluxes is therefore very important in order to adjust simulations to represent real conditions at the Dead Sea.

A periodic two stage cyclic process can describe the interaction between O_3 and BrO_x at the Dead Sea. The first stage of the process is an increase in O_3 levels, which leads to increased BrO production via Reaction (G1). This in turn leads to greater BrO_x production through Cycle 3b. This increase in BrO_x levels then leads to the depletion of O_3 during the second stage of this periodic process. During the second stage, BrO production via Reaction (G1) also decreases, due to a decrease in O_3 concentrations. This leads in turn to lower Br production due to an overall slower rate of Cycle 3b. Further decreases in Br occur due to the increase in the ratio [Br]/[BrO] for lower levels of ozone (Wayne et al., 1995), which lead to a higher rate of BrO_x termination mainly via Reactions (G4), (G17) and (G18). The resulting drop in Br concentrations weakens the O_3 depletion, and eventually O_3 starts to increase due to advection, initiating the periodic cycle once again.

If the O_3 levels drop drastically to levels below ∼1 to 2 ppbv during the second stage, further decreases in Br and BrO occur. This is due to the increased tendency of Br to form terminator species (mainly in the form of HBr), in competition with its tendency to react with O_3 (Reaction G1) at these low O_3 levels (Fig. 7). Please notice that the minimum in Br concentrations occurs around midday, simultaneously with a minimum in O_3 and a maximum in HBr concentrations (Fig. 7a). Thus, at very low O_3 levels, Br can be efficiently removed from the O_3 depletion mechanism. This strengthens the motive force of transition to the first stage, and ozone can now be transported into the area resulting in higher O_3 concentrations. This significant influence of O_3, as it drops

below ∼1 to 2 ppbv, is a major reason for the necessity of a correct treatment of its concentrations as it drops to these low levels.

The periodic process described above can also explain the observed increases in O_3 levels after dropping to levels of only few ppbv, as observed in the measurements (Fig. 2a). The model simulations without O_3 fluxes show that the observed increase in O_3 concentrations are not due to photochemical production, even at lower O_3 destruction rates by bromine activity (Fig. 2b). This strengthens the assumption that these observed increases in O_3 are the result of advected O_3.

The change of Br concentrations with time, $\frac{dBr}{dt}$, appears to play an important role in controlling the increase in O_3 concentrations due to advection. This factor changes cyclically as a part of the periodic process described previously. The second stage in this periodic process is featured by a decrease in O_3 concentrations, and a consequent decrease in BrO and Br concentrations. Thus, during the second stage of the process, $\frac{dBr}{dt}<0$ due to the O_3 depletion. The depletion of Br concentrations resulted in an increase of advected O_3 due to a lower rate of reaction with Br. This increase in O_3 due to advection is even more significant after O_3 reaches levels of below ∼1 to 2 ppbv, which lead to a more intense Br depletion, as explained above. During the first stage of this periodic process, O_3 can increase by up to a few ppb. During this stage, $\frac{dBr}{dt}>0$ due to the O_3 increase which leads to faster reactions rates via Cycle 3b. The increase in Br concentrations leads, during the second stage, to a renewed decrease in O_3 concentrations.

In this periodic process the decrease in O_3 concentrations beneath the threshold value of 1–2 ppbv, acts as a motive force for fresh O_3 fluxes to move into the evaporation ponds, initiating the production of BrO via Reaction (G1). This can explain the repeatedly observed correlation of BrO with O_3, obtained after the first depletion of O_3 during morning hours, and is the basic cause for the jagged shape of the BrO profiles at the Dead Sea evaporation ponds (Fig. 2a). The model simulations also indicate that the addition of O_3 fluxes increases the production of BrO_x, O_3 depletion rates, and paradoxically, the intensity of O_3 depletions. It is possible that incoming O_3 fluxes may

cause similar features in the diurnal profile of BrO at the margins of other locations that are larger than the area under investigation in the present study, such as the polar regions.

3.5 Factors that cause the high BrO_x production at the Dead Sea

An important question concerns the main factors which influence BrO_x production at the Dead Sea, and lead to the high BrO concentrations. Previous studies (e.g., Tas et al., 2005) hypothesized that the high measured BrO levels should be primarily attributed to the high bromine content of the water at the Dead Sea, combined with the efficient production and recycling processes of BrO_x. These studies further identified the "Bromine Explosion" mechanism as the most probable source mechanism for the gaseous bromine. In addition, the heterogeneous decomposition of $BrONO_2$ was assumed to play an important role in the recycling of RBS (Tas et al., 2005; Stutz et al., 1999). The present section discusses the relative contribution of different factors to BrO_x production at the Dead Sea.

3.5.1 Sea salt concentrations

The basic contributor to high RBS levels is an abundant source of Br^-, as is present in the Dead Sea waters. According to a laboratory study (Fickert et al., 1999) the efficiency of Br_2 release by activation of HOBr, is not expected to increase once Br^- exceeds a value of $\sim 0.8\,mol/m^3$ (for pH=5.5 and T=274°K). The Br^- at the Dead Sea exceeds this value by about two orders of magnitudes, while the Br^- of normal ocean water is about equal to this value. However, a previous study [Tas et al., 2005] has shown high frequency and high concentrations of BrO towards the more concentrated salt ponds, indicating that the high Br^- concentrations at the Dead Sea contribute to the BrO formation. Even so, the very high Br^- content may not be solely responsible for the high BrO levels observed at the Dead Sea.

3.5.2 Photochemical reactions

Model simulations showed that the formation of BrO_x is also highly dependent on photochemical reactions. This is emphasized by the similarity between the diurnal pattern of BrO_x and the photochemical decomposition rates (J values) of some bromine species that are essential for the progress of RBS activity. The sharp increase in BrO_x between 06:00 and 07:00 (Fig. 7) is mainly due to the fast increase in the rate of the photochemical decomposition of Br_2, leading to a sharp decrease in Br_2 concentrations (Fig. 6). As photochemical decomposition rates of the key bromine species reach near-zero values, the BrO_x levels decrease sharply by about 4 orders of magnitude in only 1 h, between 19:00–20:00. Although they are essential to the process, these photochemical reactions are only a necessary trigger for efficient production and recycling of RBS, as seen in the next paragraph.

3.5.3 Heterogeneous reactions

If the model is run without including heterogeneous Reactions (H1) and/or (H2), maximal BrO concentrations do not exeed 1 pptv, while the measured BrO levels were greater by about two orders of magnitude. The simulations repeatedly show that the bromine mechanism must include the two chemical processes (H1) and (H2), as illustrated in Cycle 3b, in order to obtain a good agreement between simulated and measured BrO diurnal profiles.

Another indication that Cycle 3b drives RBS activity is the relation between BrO_x concentrations and the rate of Reactions (H2) and (H1). Firstly, enhanced rates of Reaction (H2) led to increases in BrO_x concentrations, which reflect BrO_x production, because Reaction (H2) is the rate determining step in Cycle 3b. Secondly, the rate of Reaction (H2) is enhanced by Reaction (H1), leading to fast production of HOBr (Sect. 3.6). Enhanced rates of Reaction (H1) are, therefore, also associated with increases in BrO_x concentrations. In addition, BrO_x production is delayed relative to the rates of Reactions (H2) and (H1) (Fig. 8). This delay emphasizes the fact that the

production of BrO_x depends more on Reactions (H2) and (H1) than the reaction rates depend on BrO_x levels.

3.6 The role of heterogeneous processes

The heterogeneous reactions are a central component of the very fast production of BrO_x at the Dead Sea. The reason for the importance of Cycle 3b is that it leads to a nearly exponential growth of Br production via Reaction (H2) which represents the "Bromine Explosion" mechanism. Reaction (H1) has a significant influence on the rate of the "Bromine Explosion" mechanism which enhances the release of Br into the gas phase. This is because Reaction (H2) is the rate limiting step in Cycle 3b, and Reaction (H1) contributes more than other reactions to HOBr production (Reaction H1 is more efficient by a factor of ∼4 relative to Reaction G6). This can explain why the contribution of the heterogeneous Reactions (H1) and (H2) to BrO_x production and O_3 destruction is most efficient only if they appear together as in Cycle 3b.

Another effect observed at the Dead Sea that can be attributed to Reaction (H1) is the conversion of NO_2 to NO_z during RBS activity, expressed by a sharp drop in NO_2 levels concurrent with an equivalent increase of ∼1 to 2 ppb in NO_z (Fig. 9a). Measurements performed at Metzokei Dragot (Tas et al., 2005) showed that on the average for the entire campaign, NO_2 concentrations dropped to levels of below ∼0.1 ppb concentrations for BrO levels at about 30 pptv or greater, while a corresponding increase of NO_z was detected (Fig. 9a). Similarly, simulations showed that during RBS activity, NO_2 was depleted to levels of ∼0.1 ppbv together with an increase of HNO_3 (Fig. 9b). The depletion of NO_2 during RBS activity with connection to the heterogeneous decomposition of $BrONO_2$, has been reported in other field and model studies (e.g., Sander et al., 1999; Evans et al., 2003; Pszenny et al., 2004).

The model simulations show that the important chemical pathways for this conversion include the conversion of NO_2 into $BrONO_2$ and $BrNO_2$ (Reactions G14, G15) and the formation of HNO_3 by the heterogeneous decomposition of $BrONO_2$ (Reaction H1). The formation of $BrONO_2$ and $BrNO_2$ on their own can account for only ∼0.35 ppbv

(Fig. 6) of the NO_z increase, and thus cannot explain the total observed conversion. The increase in HNO_3 was shown to be anticorrelated with NO_2, in both simulations and measurements, and can account for a growth of ∼1 ppbv of NO_z (Fig. 9b). Thus, the formation of HNO_3 at the expense of NO_2 can account for the observed conversion of NO_2 into NO_z during bromine activity time. In the absence of Reaction (H1) (NOH1) (Fig. 9c), the levels of both NO_2 and HNO_3 decrease, showing that Reaction (H1) contributes significantly to the conversion of NO_2 to the more stable HNO_3. This suggests that Reaction (H1) has a significant influence on the overall balance of nitrogen oxides.

This study has shown that under conditions typical of the Dead Sea, Cycle 3b has a significant contribution to ozone destruction. The contribution of this cycle is proportional mainly to the concentrations of BrO and NO_2 and to the total surface area of substrate available for the heterogeneous Reaction (H1). Thus, the absolute contribution of Cycle 3b to ozone destruction is predicted to be smaller in areas characterized by lower levels of BrO or of NO_2 and sulfate aerosols, which are a result of less anthropogenic activity.

In order to evaluate the relative contribution of Cycle 3b to ozone destruction in other locations, it should be compared to the contributions of Cycles 1 and 2. The relative importance of each of these cycles should be evaluated based on the dependence of the rate of these cycles on BrO concentrations, which are lower in other areas. This dependence is dictated mainly by the influence of BrO concentrations on the rate of the slowest reaction in the cycle. During daytime at the Dead Sea, Reaction (H2) is the rate limiting step in Cycle 3b, slower by about two orders of magnitude relative to Reaction (G14). Since the level of BrO influences the rate of Cycle 3b only via Reaction (G14), the contribution of Cycle 3b to O_3 destruction is, on average, less than linearly dependent on BrO concentrations. As mentioned, Cycle 1 has a quadratic dependence on BrO concentrations, while the dependence of Cycle 2 is linear. Thus, under the Dead Sea conditions the dependence of BrO_x production and O_3 destruction on BrO concentrations via Cycle 3b is lower than those of Cycles 1 and 2. Therefore, in the boundary layer at other mid-latitude areas under anthropogenic influence, char-

acterized by similar levels of NO_2 and sulfate aerosols and by lower BrO levels, the relative contribution of Cycle 3b to O_3 destruction may be similar or even higher than the contribution at the Dead Sea. However, in areas that are influenced by lower anthropogenic activity, and are characterized by lower levels of sulfate aerosols and NO_2, the relative contribution of Cycle 3b is predicted to be smaller than at the Dead Sea.

The model simulations showed that the heterogeneous decomposition of $BrONO_2$ (Reaction H1) is of crucial importance to ozone destruction through the production of BrO_x via Cycle 3b and the recycling of BrO_x by Cycle 3a. Under the Dead Sea conditions the influence of the heterogeneous decomposition of $BrONO_2$ via Cycle 3b is slightly less than linearly dependent on BrO and NO_2 concentrations, similarily to what was previously shown. Thus, both the absolute and relative importance of this chemical process may become much smaller at areas that are not under significant influence of anthropogenic activity. The same dependence on anthropogenic activity should be attributed to the influence of the heterogeneous decomposition of $BrONO_2$ on BrO_x recycling via Cycle 3a. This is due to the less-than-linear dependence of this cycle on the rate of Reaction (G14), under the Dead Sea conditions, reflecting the fact that the rate of Reaction (H1) is slower by a factor of ~2.5 than the rate of Reaction (G14).

The analysis described in this paper shows that the production and recycling of BrO_x, and the consequent destruction of ozone, should be proportional to ambient concentrations of NO_2 and sulfate aerosols. Since the levels of NO_2 vary significantly with the distance from pollution sources, the influence of the heterogeneous decomposition of $BrONO_2$ on BrO_x production via Cycle 3b and BrO_x recycling via Cycle 3a should be checked under different levels of NO_2. This subject will be investigated in a later paper.

4 Conclusions

This paper presents a chemical mechanism that can describe the RBS activity at the Dead Sea. It was shown that the model must include advected ozone fluxes and het-

erogeneous processes in order to duplicate the measurements. The present study indicates that the extraordinarily high BrO levels that were measured at the Dead Sea can only partially be associated with the high Br^- content at the Dead Sea. These high levels may be attributed also to highly efficient heterogeneous processes of recycling and production that occur in the area. The two heterogeneous processes that were included are (1) the release of Br^- into the gas phase via the "Bromine Explosion" mechanism which occurs in sea salt aerosols and (2) the decomposition of $BrONO_2$ that occurs on the surface area of sulfate aerosols. These processes, only if included together as illustrated in Cycle 3b, can account for the efficient BrO_x production and O_3 destruction at the Dead Sea.

The heterogeneous decomposition of $BrONO_2$ at the Dead Sea is an essential link in the production of BrO_x since it leads to the production of HOBr ~4 times faster than its production in homogeneous gas phase (Reaction G6). The HOBr may then activate the release of Br into the gas phase by the "Bromine Explosion" mechanism, or else undergo a fast photolysis to yield Br. It should also be noted that model simulations indicate that the release of Br_2 by activation of HOBr may also occur directly from the sea water or salt pans and not only from the sea salt aerosols.

The present research focused on a chemical cycle which includes both the "Bromine Explosion" mechanism and the heterogeneous decomposition of $BrONO_2$ (Cycle 3b). Under the Dead Sea conditions, this cycle was found to dramatically enhance the ozone destruction rate via BrO_x production, and control the diurnal profiles of Br and BrO. The absolute contribution of this cycle to the destruction of ozone may be less in the boundary layer at other regions characterized by lower levels of BrO or lower anthropogenic activity, due to lower levels of NO_2 and lower sulfate aerosols levels. In these areas, both the absolute and relative contribution of the heterogeneous decomposition of $BrONO_2$ to ozone destruction via Cycle 3b is predicted to be smaller. In contrast, the relative contribution of Cycle 3b may be higher in areas that are under anthropogenic influence but are characterized by lower BrO levels. Variations in anthropogenic activity affect Cycle 3b mainly by the levels of NO_2 and, to a lesser extent,

by the levels of sulfate aerosols. This is because NO_2 levels are more sensitive to the distance from pollution sources. The influence of NO_2 levels on the rate of the heterogeneous decomposition of $BrONO_2$ and the consequent rate of BrO_x production and ozone destruction will be presented in a later paper.

The heterogeneous decomposition of $BrONO_2$ during RBS activity leads to an increase in the concentrations of HNO_3 which is anticorrelated with NO_2 concentrations and causes NO_2 to decrease to levels of below ∼0.1 ppbv. This finding can account for the measured increase in NO_z concentrations that occurs simultaneously with a decrease in NO_2 during RBS activity, an effect which cannot be explained solely by the formation of $BrONO_2$ and $BrNO_2$.

Ozone is a limiting factor to BrO_x production and O_3 destruction at the Dead Sea evaporation ponds, since O_3 frequently reaches levels of below ∼1 to 2 ppbv. The flow of O_3 fluxes into the Dead Sea evaporation ponds was found to be essential for the continuation of RBS activity and O_3 destruction, especially after O_3 reached threshold levels below ∼1 to 2 ppb. This flow of O_3 fluxes enables the enhancement of BrO_x production and leads to a higher rate of O_3 destruction. There is a high probability that the changes in Br concentrations with time serve as a chemical regulator for the entrainment of O_3 fluxes, in a way that promotes the entrainment of O_3 fluxes as O_3 levels reach low enough levels. This chemical pattern accounts both for the jagged shape of BrO profile and the correlation between O_3 and BrO, as O_3 reaches low enough levels. Similar features in the diurnal profile of BrO and its relation to O_3 may also be detected at the margins of regions exhibiting RBS activity which are much larger in area than the Dead Sea.

An important conclusion of this study is that a homogeneous gas phase mechanism is not sufficient to describe the RBS activity at the Dead Sea. The two heterogeneous processes, the decomposition of $BrONO_2$ and the "Bromine Explosion" mechanism, have a major contribution to the overall activity of RBS in the Dead Sea area, and are sufficient to account for this activity when combined with the gas phase reactions. The heterogeneous decomposition of $BrONO_2$ plays a major role in the interaction between

bromine species and NO_2. A later paper will focus on this process and its importance in this interaction and the consequent destruction of O_3. Further investigation of RBS activity at the Dead Sea should include a more detailed description of the interaction between bromine species and anthropogenic NO_2. This may be especially important in order to obtain a more accurate knowledge of the RBS activity at mid-lattitudes.

References

Aranda, A., Bras, G. L., LaVerdet, G., and Poulet, G.: The BrO+CH3O2 reaction: kinetics and role in the atmospheric ozone budget, Geophys. Res. Lett., 24, 2745–2748, 1997.

Andreae, T. W., Andreae, M. O., Ichoku, C., Maenhaut, W., Cafmeyer, J., Karnieli, A., and Orlovsky, L.: Light scattering by dust and anthropogenic aerosol at remote site in the Negev desert, Israel, J. Geophys. Res, 107(D2), 4008, doi:10.1029/2001JD900252, 2002.

Atkinson, R., Baulch, D. L., Cox, R. A., Crowley, J. N, Hampson, R. F., Kerr, J. A., Rossi, M. J., and Troe, J.: Summary of Evaluated Kinetic and Photochemical Data for Atmospheric Chemistry, IUPAC Subcommittee on Gas Kinetic Data Evaluation for Atmospheric Chemistry, Web Version http://www.iupac-kinetic.ch.cam.ac.uk/, 2002.

Barrie, L. A. and Platt, U.: Arctic tropospheric chemistry: an overview, Tellus, 49B(5), 450–454, 1997.

Atkinson, R., Baulch, D. L., Cox, R. A., Crowley, J. N, Hampson, R. F., Kerr, J. A., Rossi, M. J., and Troe, J.: Summary of Evaluated Kinetic and Photochemical Data for Atmospheric Chemistry, IUPAC Subcommittee on Gas Kinetic Data Evaluation for Atmospheric Chemistry, Web Version http://www.iupac-kinetic.ch.cam.ac.uk/, 2003.

Atkinson, R., Baulch, D. L., Cox, R. A., Crowley, J. N., Hampson, R. F, Kerr, J. A., Rossi, M. J., and Troe, J.: Summary of Evaluated Kinetic and Photochemical Data for Atmospheric Chemistry, IUPAC Subcommittee on Gas Kinetic Data Evaluation for Atmospheric Chemistry, Web Version http://www.iupac-kinetic.ch.cam.ac.uk/, 2004.

Barrie, L. A., Bottenheim, J. W., Schnell, R. C., Crutzen, P. J., and Rasmussen, R. A.: Ozone destruction and photochemical reactions at polar sunrise in the lower Arctic atmosphere, Nature, 334, 138–141, 1988.

Bedjanian, Y., Riffault, V., Le Bras, G., and Poulet, G.: Kinetics and Mechanism of the OH and OD Reactions with BrO, J. Phys. Chem. A, 105, 6154–6166, 2001.

Beine, H. J., Jaffe, D. A., Stordal F., Engardt, M., Solberg, S., Schmidbauer, N., and Holmen, K.: NOx during ozone depletion events in the arctic troposphere at NY-Alesund, Svalbard, Tellus, 494, 556–565, 1997.

Bloss, W. J., Rowley, D. M., Cox, R. A., and Jones, L. J.: Rate coefficient for the BrO+HO2 raction at 298 K, Phys. Chem. Chem. Phys, 4(15), 3639–3647, 2002.

Evans, M. J., Jacob, D. J., Atlas, E., Cantrell, C. A., Eisele, F., Flocke, F., Fried, A., Mauldin, R. L., Ridley, B. A., Wert, B., Talbot, R., Blake, D., Heikes, B., Snow, J., Welega, J., Weinheimer, A. J., and Dibb, J.: Coupled evolution of BrOX-ClOX-HOX-NOX chemistry during bromine-catalyzed ozone depletion events in the arctic boundary layer, J. Geophys. Res., 108(D4), 8368, doi:10.1029/2002JD002732, 2003.

Fan, S.-M. and Jacob, D. J.: Surface ozone depletion in Arctic spring sustained by bromine reactions on aerosols, Nature, 359, 522–524, 1992.

Fickert, S., Adams, J. W., and Crowley, J. N.: Activation of Br_2 and BrCl via uptake of HOBr onto aqueous salt solutions, J. Geophys. Res., 104(D19), 23 719–23 727, 1999.

Formenti, P., Andrea, M. O., Andrea, T. W., Ichoku, C., Schebeske G., Kettle, J., Maenhaut, W., Ptasinsky, J., Karnieli A., and Leliveld, J.: Physical and chemical characteristics of aerosols over the Negev Desert (Israel) during summer 1996, J. Geophys. Res., 106(D5), 4871–4890, 2001.

Gilles, M. K., McCabe, D. C., Burkholder, J. B., and Ravishankara, A. R.: Measurement of the Rate Coefficient for the Reaction of OH with BrO, J. Phys. Chem. A., 105, 5849–5853, 2001.

Gong, S. L., Barrie, L. A., and Blanchey, J.-P.: Modeling sea-salt aerosols in the atmosphere 1. Model development, J. Geophys. Res., 102(D3), 3805–3818, 1997.

Gras, J. L. and Ayers, G. P.: marine aerosol at southern mid-latitudes, J. Geophys. Res., 88(C15), 10 661–10 666, 1983.

Hanson, D. R. and Ravishankara, A. R.: Heterogeneous chemistry of Bromine species in sulfuric acid under stratospheric conditions, J. Geophys. Res., 22(4), 385–388, 1995.

Hanson, D. R., Ravishankara, A. R., and Lovejoy, E. R.: Reaction of $BrONO_2$ with H_2O on submicron sulfuric acid aerosol and implications for the lower stratosphere, J. Geophys. Res., 101(D4), 9063–9069, 1996.

Harwood, M. H. and Burkholder, J. B.: Photodissociation of $BrONO_2$ and N_2O_5: Quantum yields for NO_3 production at 248, 308, and 352.5 nm, J. Phys. Chem. A., 102(8), 1309–1317, 1998.

Hausmann, M. and Platt, U.: Spectroscopic measurement of bromine oxide and ozone in

the high Arctic during Polar Sunrise Experiment 1992, J. Geophys. Res., 99(25), 399–413, 1994.

Hebestreit, K., Stutz, J., Rosen, D., Matveev, V., Peleg, M., Luria, M., and Platt, U.: First DOAS Measurements of Tropospheric Bromine Oxide in Mid Latitudes, Science, 283, 55–57, 1999.

Honninger, G., Bobrowski, N., Palenque, E. R., Torrez, R., and Platt, U.: Reactive bromine and sulfur emissions at Salar de Uyuni, Bolivia, Geophys. Res. Lett., 31, L04101, doi:10.1029/2003GL018818, 2004.

Kreher, K., Johnston, P. V., Wood, S. W., Nardi, B., and Platt, U.: Ground-based measurements of tropospheric and stratospheric BrO at Arrival Heights (78° S), Antarctica, Geophys. Res. Lett., 24(23), 3021–3024, 1997.

Leser, H., Honinger, G., and Platt, U.: Max-DOAS measurements of BrO and NO_2 in the marine boundary layer, Geophys. Res. Lett., 31, 1537, doi:10.1029/2002GL015811, 2003.

Li, Z. and Tao, Z.: A kinetic study on reactions of OBrO with NO, OClO, and ClO at 298 K, Chem. Phys. Lett., 306, 17–123,1999.

Madronich, S. and Flocke, S.: The role of solar radiation in atmospheric chemistry, in: Handbook of Environmental Chemistry, edited by: Boule, P., Springer-Verlag, Heidelberg, 1–26, 1998.

Matveev, V., Hebestreit, K., Peleg, M., Rosen, D. S., Tov-Alper, D., Stutz, J., Platt, U., Blake, D., and Luria, M.: Bromine Oxide-Ozone interaction over the Dead Sea, J. Geophys. Res., 106, D10, 10 375–10 387, 2001.

McNider, R. T. and Pielke, R. A.: Diurnal boundary-layer development over sloping terrain, J. Atmos. Sci., 38, 2198–2212, 1981.

Mozurkewich, M.: Mechanisms for the release of halogens from sea-salt particles by free radical reactions, J. Geophys. Res., 100(D7), 14 199–14 207, 1995.

Murayama, S., Nakazawa, T., Tanaka, M., Aoki, S., and Kawaguchi, S.: Variations of tropospheric ozone concentration over Syowa Station, Antarctica, Tellus, 44B, 262–272, 1992.

Niemi, T. M., Ben-Avraham, Z., and Gat, J. R.: The Dead Sea: The Lake and Its Setting, Oxford Monogr. Geol. Geophys., vol. 36, Oxford Univ. Press, New York, 1997.

Platt, U. and Honninger, G.: The role of halogen species in the troposphere, Chemosphere, 52, 325–358, 2003.

Platt, U. and Moortgat, G. K.: Heterogeneous and Homogeneous Chemistry of Reactive Halogen Compounds in the Lower Troposphere, J. Atmos. Chem., 34, 1–8, 1999.

Pour Biazar, A.: The role of natural nitrogen oxides in ozone production in the southern environ-

ment, Dissertation, The Department of Atmospheric Sciences, The University of Alabama in Huntsville, 1995.

Pszenny, A. A. P., Moldanova, J., Keene, W. C., Sander, R., Maben, J. R., Martinez, M., and Crutzen, P. J.: Halogen cycling and aerosol pH in the Hawaiian marine boundary layer, Atmos. Chem. Phys., 4, 147–168, 2004.

Ridley, B. A. and Orlando, J. J.: Active Nitrogen Surface Ozone Depletion Events at Alert during Spring 1998, J. Atmos. Chem., 44, 1–22, 2003.

Sander, R. and Crutzen, P. J.: Model study indicating halogen activation and ozone destruction in polluted air masses transported to the sea, J. Geophys. Res., 101(D4), 9121–9138, 1996.

Sander, R., Rudich, Y., and von Glasow, R.: The role of BrNO3 in marine tropospheric chemistry: A model study, Geophys. Res. Lett., 26(18), 2857–2860, 1999.

Sander, R., Rudich, Y., Von Glasow, R., and Crutzen, P. J.: The role of $BrNO_3$ in marine tropospheric chemistry: A model study, J. Geophys. Res., 26(18), 2857–2860, 2003.

Stutz, J., Hebestreit, K., Alicke, B., and Platt, U.: Chemistry of halogen oxides in the troposphere: comparison of model calculations with recent field data, J. Atmos. Chem., 34, 65–85, 1999.

Stutz, J., Ackermann, R., Fast, J. D., and Barrie, L.: Atmospheric reactive chlorine and bromine at the Great Salt Lake, Utah, Geophys. Res. Lett., 29, 1380, doi:10.1029/2002GL014812, 2002.

Sverdrup, H. U., Johnson, M. W., and Fleming, R. H.: The Oceans, Their Physics, Chemistry and General Biology, Prentice-Hal, Englewood Cliffs, N. J., 1942.

Tang, T. and McConnell, J. C.: Autocatalytic release of bromine from Arctic snow pack during polar sunrise, Geophys. Res. Lett., 23(19), 2633–2636, 1996.

Tas, E., Matveev, V., Zingler, J., Luria, M., and Peleg, M.: Frequency and extent of ozone destruction episodes over the Dead Sea, Israel, Atmos. Environ., 37(34), 4769–4780, 2003.

Tas, E., Peleg, M., Matveev, V., Zingler, J., and Luria, M.: Frequency and extent of bromine oxide formation over the Dead Sea, J. Geophys. Res., 110(D11), D11304, doi:10.1029/2004JD005665, 2005.

Trainer, M., Williams, E. J., Parish, D. D., Buhr, M. P., Allwine, E. J., Westberg, H. H., Fehsenfeld, F. C., and Liu, S. C.: Models and observations of the impact of natural hydrocarbons on rural ozone, Nature, 329, 705–707, 1987.

Tuckermann, M., Ackermann, R., Golz, C., Lorenzen-Schmidt, H., Senne, T., Stutz, J., Trost, B., Unold, W., and Platt, U.: DOAS-Observation of Halogen Radical-catalysed Arctic Boundary

Layer Ozone Destruction During the ARCTOC-Campaigns 1995 and 1996 in Ny-Alesund, Spitsbergen, Tellus, 49B, 533–555, 1997.

Vogt, R., Crutzen, P. J., and Sander, R.: A mechanism for halogen release from sea-salt aerosol in the remote marine boundary layer, Nature, 383, 327–330, 1996.

Von Glasow, R., Sander, R., Bott, A., and Crutzen, P. J.: Modeling halogen chemistry in the marine boundary layer 1. Cload-free MBL, J. Geophys. Res., 107, 4341, doi:10.1029/2001JD000942, 2002.

Von Glasow, R., von Kuhlman, R., Lawrence, M. G., Platt, U., and Crutzen, P. J.: Impact of reactive bromine chemistry in the troposphere, Atmos. Chem. Phys., 4, 2481–2497, 2004.

Wanger, A., Peleg, M., Sharf, G., Mahrer, Y., Dayan, U., Kallos, G., Kotroni, V., Lagouvardos, K., Varinou, M., Papadopoulos, A., and Luria, M.: Some observational and modeling evidence of long-range transport of air pollutants from Europe toward Israeli coast, J. Geophys. Res., 105(D6), 7177–7186, 2000.

Wayne, R. P., Poulet, G., Biggs, P., Burrows, J. P., Cox, R. A., Crutzen, P. J., Haymann, G. D., Jenkin, M. E., Bras, G. L., Moortgat, G. K., Platt, U., and Schindler, R. N.: Halogen oxides: radicals, sources and reservoirs in the laboratory and in the atmosphere, Atmos. Environ., 29, 2675–2884, 1995.

Zingler, J. and Platt, U.: Iodine oxide in the Dead Sea Valley: Evidence for inorganic sources of boundary layer IO, J. Geophys. Res., 110, D07307, doi:10.1029/2004JD004993, 2005.

Table 1. Reactions in the gas phase.

Reaction no.	Gas phase reactions	Rate constant (cm^3 $molecules^{-1}s^{-1}$)	Reference
G1	$Br+O_3 \rightarrow BrO+O_2$	$1.2 \cdot 10^{-12}$	1
G2	$BrO+BrO \rightarrow Br+Br+O_2$	$2.7 \cdot 10^{-12}$	1
G3	$BrO+BrO \rightarrow Br_2+O_2$	$4.8 \cdot 10^{-13}$	1
G4	$Br+HO_2 \rightarrow HBr+O_2$	$2.0 \cdot 10^{-12}$	1
G5	$BrO+HO_2 \rightarrow HBr+O_3$	$2.3 \cdot 10^{-13}$	1, 2
G6	$BrO+HO_2 \rightarrow HOBr+O_2$	$2.3 \cdot 10^{-11}$	1, 2
G7	$BrO+OH \rightarrow Br+HO_2$	$4.1 \cdot 10^{-11}$	3, 4, 5
G8	$BrO+OH \rightarrow HBr+O_2$	$4.1 \cdot 10^{-13}$	3
G9	$Br_2+OH \rightarrow HOBr+Br$	$4.5 \cdot 10^{-11}$	1
G10	$HBr+OH \rightarrow H_2O+Br$	$1.1 \cdot 10^{-11}$	1
G11	$Br+NO_3 \rightarrow BrO+NO_2$	$1.6 \cdot 10^{-11}$	1
G12	$BrO+NO_3 \rightarrow BrOO+NO_2$	$1.0 \cdot 10^{-12}$	1
G13	$OBrO+NO \rightarrow BrO+NO_2$	$1.8 \cdot 10^{-12}$	6
G14	$BrO+NO_2 \xrightarrow{M} BrONO_2^a$	$5.7 \cdot 10^{-12}$	1
G15	$Br+NO_2 \xrightarrow{M} BrNO_2^a$	$6.5 \cdot 10^{-12}$	1
G16	$BrO+NO \rightarrow Br+NO_2$	$2.1 \cdot 10^{-11}$	1
G17	$Br+CH_2O \rightarrow HBr+HCO$	$1.1 \cdot 10^{-12}$	1
G18	$Br+C_2H_2 \rightarrow CH_2Br$	$2.6 \cdot 10^{-14}$	1
G19	$Br+C_2H_4 \rightarrow BrC_2H_4$	$1.3 \cdot 10^{-13}$	1
G20	$Br+CH_3CHO \rightarrow HBr+CH_3CO$	$3.9 \cdot 10^{-12}$	1
G21	$Br+CH_3O_2 \rightarrow BrO+CH_3O$	$2.5 \cdot 10^{-14}$	7
G22	$Br+C_3H_6 \rightarrow HBr+C_3H_5^b$	$1.2 \cdot 10^{-14}$	1
G23	$Br+C_3H_6 \xrightarrow{M} BrC_3H_6^b$	$3.6 \cdot 10^{-12}$	1
G24	$BrO+CH_3O_2 \rightarrow Br+CH_3O+O_2$	$0.9 \cdot 10^{-12}$	8
G25	$BrO+CH_3O_2 \rightarrow OBrO+CH_3O$	$0.9 \cdot 10^{-12}$	8
G26	$BrO+CH_3O_2 \rightarrow HOBr+CH_2O_2$	$4.6 \cdot 10^{-12}$	8

[1] Atkinson et al. (2003); [2] Bloss et al. (2002); [3] Bedjanian et al. (2001); [4] Gilles et al. (2001); [5] Atkinson et al. (2004); [6] Li and Tao (1999); [7] Stutz et al. (1999); [8] Aranda et al. (1997);
[a] Pressure dependent reactions; Calculated for 800 mm Hg and 305 K.
[b] Insignificant

Table 2. Photolysis of Bromine species reactions and their average daytime rate constants in the gas phase calculated for 15° zenith angle and clear sky at the Dead Sea (31.0° latitude).

Reaction No.	Gas phase reactions	Gas phase reactions	Reference
GP1	$Br_2 \xrightarrow{h\nu} Br+Br$	$3.1 \cdot 10^{-02}$	1
GP2	$BrO \xrightarrow{h\nu} Br+O_3$	$3.8 \cdot 10^{-02}$	1
GP3	$HOBr \xrightarrow{h\nu} Br+OH$	$2.5 \cdot 10^{-03}$	1
GP4	$BrONO_2 \xrightarrow{h\nu} Br+NO_3$	$1.6 \cdot 10^{-03}$	2
GP5	$BrNO_2 \xrightarrow{h\nu} Br+NO_2^a$	$2.2 \cdot 10^{-03}$	3
GP5	$OBrO \xrightarrow{h\nu} BrO+O_3$	$1.3 \cdot 10^{-00}$	1

[1] Atkinson (2003); [2] Atkinson et al. (2002); ϕ was taken from Harwood et al. (1998); [3] Stutz et al. (1999); [a] Estimated from red-shifted ClONO absorption cross-section by 50 nm.

Table 3. Deposition velocities for some bromine species.

Species	v_d cms^{-1}
HOBr	0.2 [a]
HBr	0.65 [a]
$BrONO_2$	0.18 [b]
$BrNO_2$	0.18 [b]

[a] Values were determined based on Sander and Crutzen (1996).
[b] Values similar to those of NO_2 were used.

Table 4. Key of different simulation runs.

Simulation	Individual conditions for calculations[a]
"FULL"	Full bromine species mechanism as described later in Sects. 2.1, 3.4.
"NOB"	No bromine mechanisms included.
"NOOZ"	No O_3 fluxes advected during RBS activity. O_3 fluxes advected only for a short time during evening when RBS activity was insignificant.
"NOHET"	No heterogeneous reactions included[b].
"NOH1"	Reaction (H1) was excluded[c].
"NOH2"	Reaction (H2) was excluded[c].
"NWS"	Wind speed parameterization not included for Reaction (H2). The rate of Reaction (H2) was normalized in order to obtain the same daily average value that was used in the "FULL" simulation.
"NWD"	Wind direction parameterization for Reaction (H2) was not included. The rate of Reaction (H2) was normalized in order to obtain the same daily average value that was used in the "FULL" simulation.

[a] All simulation except for NOHET, NOH1 and NOH2 were run with a maximal Br_2 flux of 10 molecules cm^{-2} s^{-1} normalized to the actinic flux at the area at the appropriate time.
[b] Simulation with maximal Br_2 flux of $5{\cdot}10^{10}$ molecules·cm^{-2}·s^{-1} normalized to the actinic flux at the appropriate time.
[c] Simulation with maximal Br_2 flux of 10^{10} molecules·cm^{-2}·s^{-1} normalized to the actinic flux at the appropriate time.

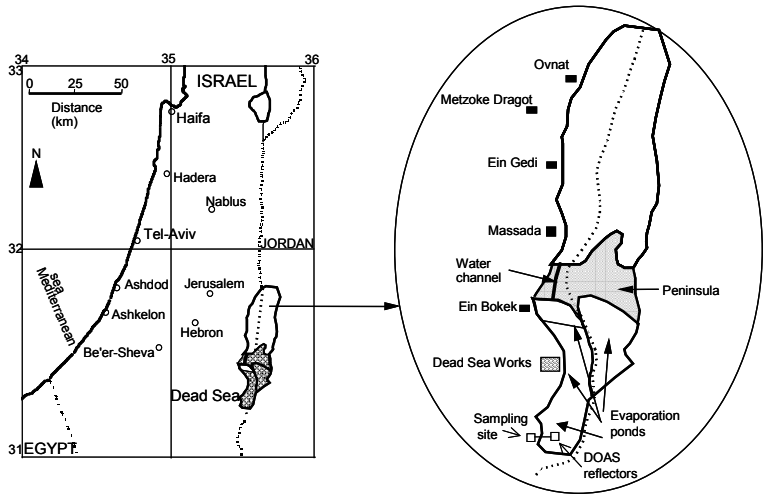

Fig. 1. Map of Israel, inset showing Dead Sea region.

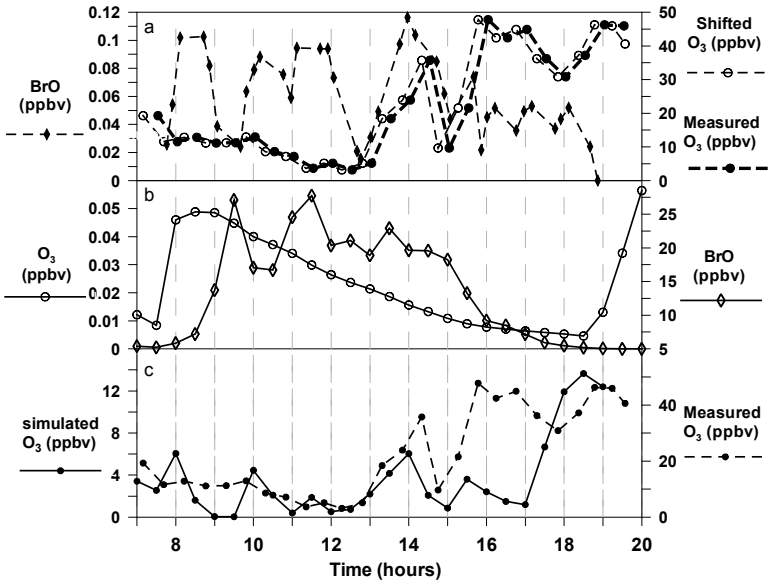

Fig. 2. Movement of ozone fluxes into the spatial region of bromine activity. **(a)** Measured BrO concentrations vs. time-shifted and not shifted measured O_3 concentrations during Julian day 221. **(b)** BrO and O_3 concentrations for "NOOZ" simulation. Simulated BrO and O_3 concentrations did not match the measured levels when O_3 fluxes were not added **(c)** Model O_3 concentrations vs. measured (time-shifted). It appears evident that the jagged events in the BrO profile are associated with times when modeled O_3 crosses the threshold value of ∼1 to 2 ppb (panels a and c).

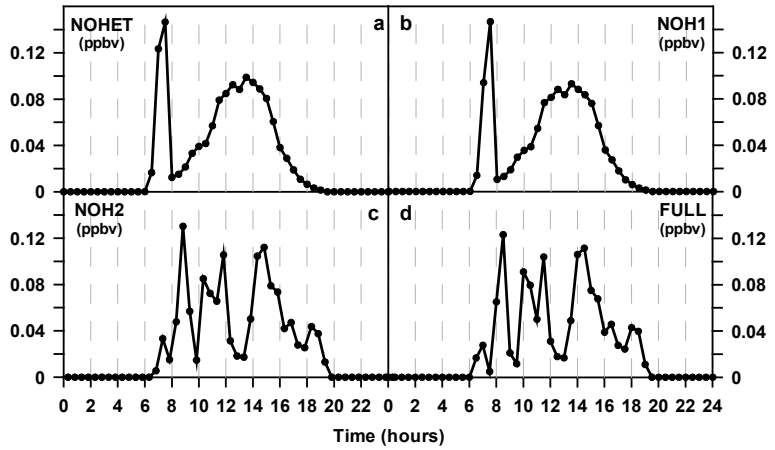

Fig. 3. Diurnal profiles of BrO obtained in different simulations (see Table 4 for the conditions of each simulation).
(a) NOHET – Heterogeneos reactions (Reactions H1 and H2) are not included
(b) NOH1 – Reaction (H1) is not included
(c) NOH2 – Reaction (H2) is not included
(d) FULL – All reactions are included
In plots (a), (b) and (c), the Br_2 flux was multiplied by $\sim 10^9$ (Table 4). Reaction (H1) is necessary for the structure, Reaction (H2) is necessary for the magnitude of BrO concentrations.

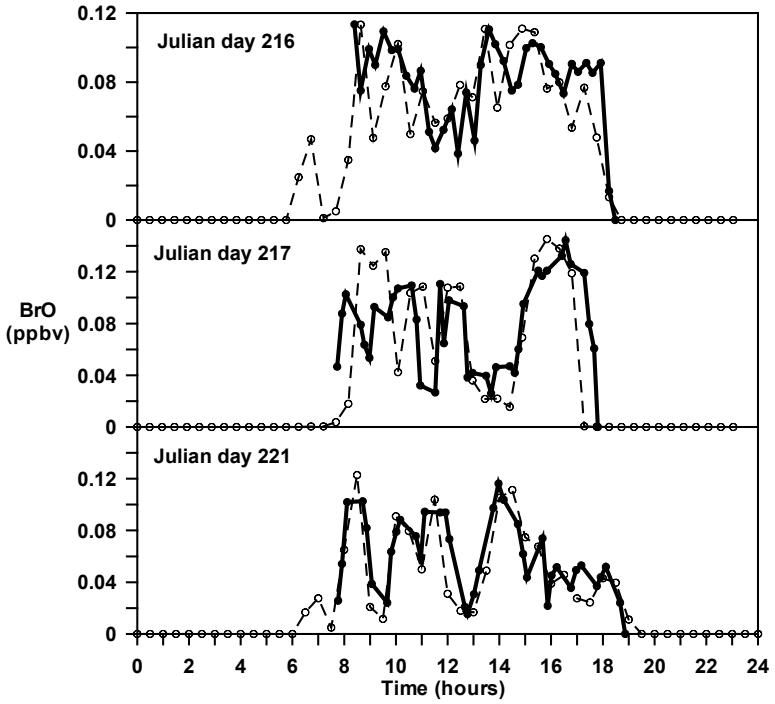

Fig. 4. Comparison between measured and simulated BrO. This graph presents only measurements of BrO concentrations above 20 pptv.

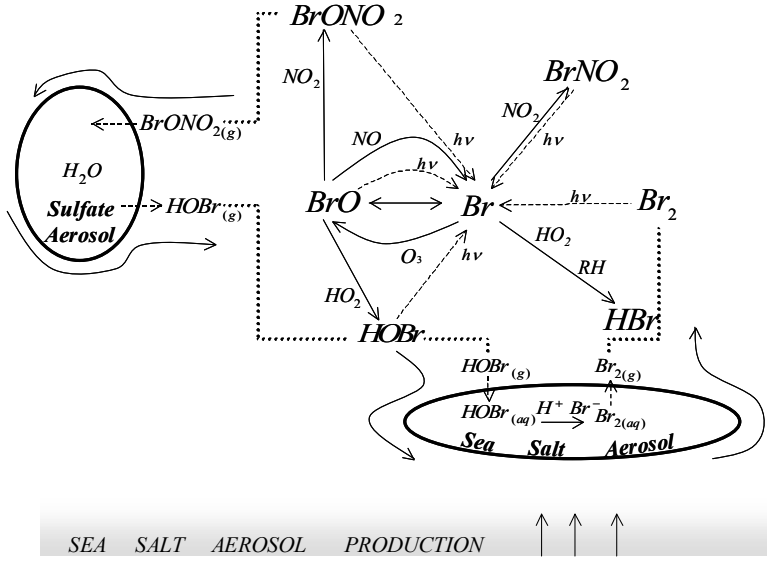

Fig. 5. Schematic description of the RBS mechanism that was used in the model.

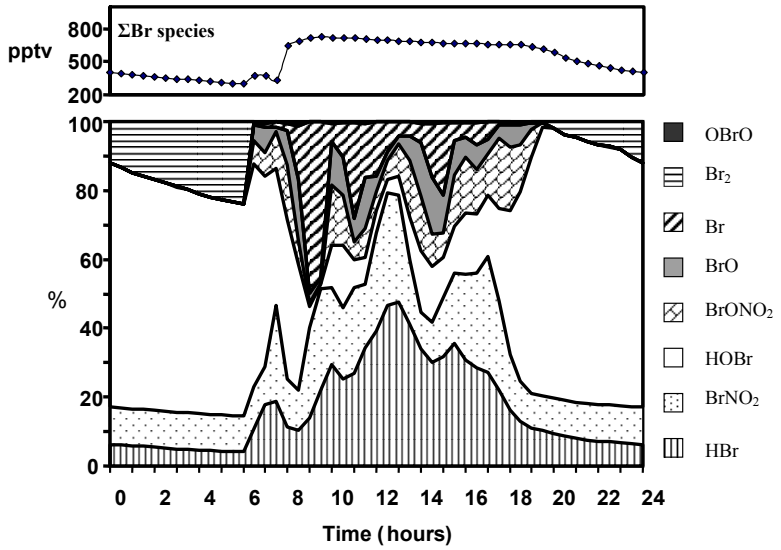

Fig. 6. Cumulative diurnal profile of significant bromine species. "ΣBr species" refers to the sum of the 8 bromine species shown in the lower panel.

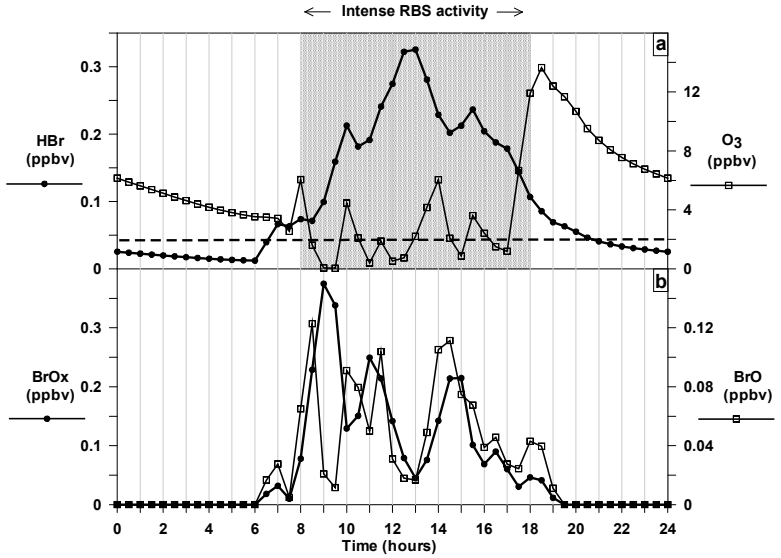

Fig. 7. The influence of O_3 depletion below ∼1–2 ppbv on Br and BrO diurnal profiles. **(a)** When O_3 levels were dropped below ∼1–2 ppbv (dashed line at 2 ppbv),concentrations of HBr increased, indicating an increase in the rate that Br undergoes termination reactions. **(b)** This in turn causes the decrease in Br and BrO concentrations, and hence leads to lower BrO_x levels.

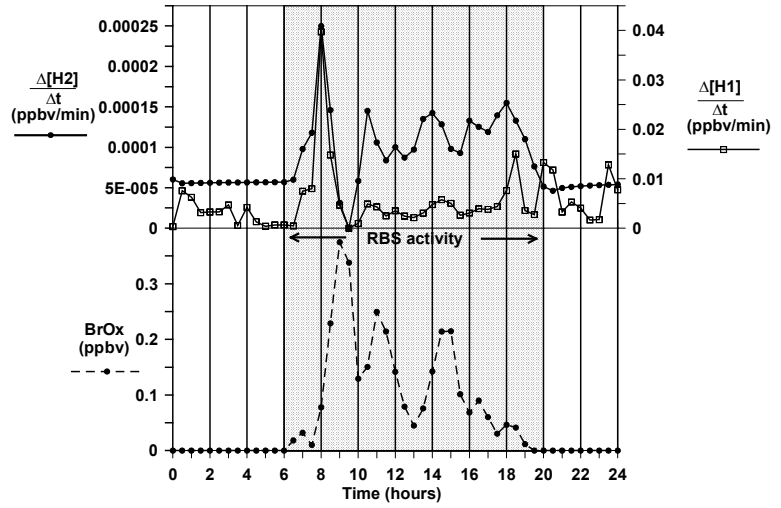

Fig. 8. The dependence of BrOx production on the heterogeneous processes. During RBS activity (shaded area) there is a correlation (r=0.73) between the trends in the rates of Reactions (H2) and (H1). Enhanced rates of these reactions led to increases in BrO_x concentrations (which reflect BrO_x production). This is because Reaction (H2) is the rate determining step in Cycle 3b and is enhanced by Reaction (H1). The BrO_x concentrations exhibit a correlation with these reaction rates, subject to a delay on the order of ∼1/2 h, which is the model time resolution of the output.

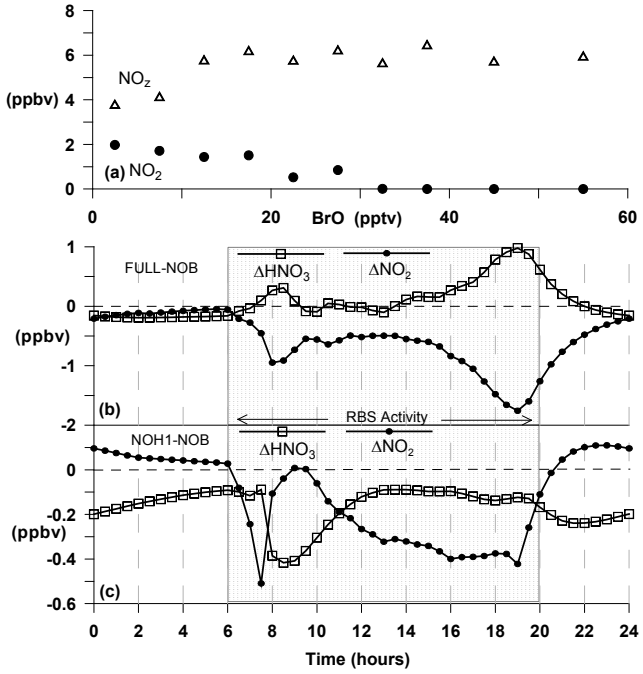

Fig. 9. Comparison of NO_2 and NO_z by measurements and simulations. The influence of BrO on NO_2 and NOz at Metzokei Dragot is shown. Values were averaged over the entire campaign period and are presented in bins **(a)**. ΔHNO_3: HNO_3 concentrations during a simulation that includes bromine species (i.e, "FULL" in **(b)** and "NOH1" in **(c)**) minus HNO_3 concentrations during "NOB" simulation. ΔNO_2: NO_2 concentrations during a simulation that includes bromine species (i.e., "FULL" in (b) and "NOH1" in (c)) minus NO_2 concentrations during "NOB" simulation.